Available online at www.sciencedirect.com

SciVerse ScienceDirect

journal homepage: www.elsevier.com/locate/he

Synthesis and characterization of new sulfonated polytriazole proton exchange membrane by click reaction for direct methanol fuel cells (DMFCs)

Yao Jheng Huang [a], Yun Sheng Ye [b], Ying Chieh Yen [a], Li Duan Tsai [a], Bing Joe Hwang [b], Feng Chih Chang [a,*]

[a] Institute of Applied Chemistry, National Chiao-Tung University, Hsin-Chu, Taiwan
[b] Department of Chemical Engineering, National Taiwan University of Science and Technology, Taipei, Taiwan

ARTICLE INFO

Article history:
Received 22 April 2011
Received in revised form
24 August 2011
Accepted 29 August 2011
Available online 22 September 2011

Keywords:
Sulfonated polytriazole
Click chemistry
Proton exchange membrane
Acid-base interaction

ABSTRACT

Sulfonated polytriazole (SPTA) in which the acidic sulfonic acid and basic triazole groups act as physical crosslinking sites within a polymer backbone has been successfully prepared, for use as a proton exchange membrane, using the click reaction. The acid-base interactions of the SPTA membranes leads to the formation of well-dispersed ionic clusters and the random distribution of ion channels with good connectivity resulting in lower methanol permeabilities at ambient temperatures and similar or higher proton conductivities than Nafion 117 at 80 °C in conditions of near zero relative humidity. Proton conductivities (σ) of 0.149 S cm^{-1} at 80 °C and 9 × 10^{-5} S cm^{-1} in anhydrous conditions together with low methanol permeability (P) at 0.1 × 10^{-6} cm^2 s^{-1} that are comparable or superior to Nafion 117 ($\sigma_{T=80}$: 0.151 S cm^{-1}; $\sigma_{RH=0}$: 3 × 10^{-5} S cm^{-1}; $P_{T=30}$: 1.31 × 10^{-6} cm^2 s^{-1}) were achieved. Additionally, the selectivity of SPTA is approximately four times higher than that of Nafion 117, thus it may have potential for use in direct methanol fuel cells (DMFCs).

1. Introduction

Direct methanol fuel cells (DMFCs) are attractive as a power source because of their high energy density, high energy conversion efficiency and because they do not require an electrical outlet for recharging. Additionally, they are easy to refuel and are easily incorporated in systems design. There is a wide range of potential uses, including stationary, portable and automotive applications for polymer electrolyte membrane fuel cells (PEMFCs) [1]. Proton exchange membranes (PEMs) are key components of PEMFCs that provide an ionic pathway for proton transfer while preventing mixing of the reactant gases [1,2]. The perfluorosulfonic acid ionomer Nafion® is one of the most studied solid polymer electrolyte membranes because of its chemical and physical stability at moderate temperatures and its high proton conductivity that arises from its nanophase-separated morphology and highly interconnected ionic channels [3]. There are however, several drawbacks that limit Nafion's application including: high cost, high methanol permeability, and incompatibility with other materials [2]. Among the various types of fuel cell PEMs, several non-fluorinated polymeric materials are attracting attention as alternatives to perfluorinated polymer membranes because of

* *Corresponding author*. Tel./fax: +886 3 5131512.
E-mail address: changfc@mail.nctu.edu.tw (F.C. Chang).

0360-3199/$ – see front matter Copyright © 2011, Hydrogen Energy Publications, LLC. Published by Elsevier Ltd. All rights reserved.
doi:10.1016/j.ijhydene.2011.08.093

their advantages in terms of cost, safety, ease of synthesis and structural diversity [4]. A large number of PEMs has recently been prepared from sulfonated aromatic hydrocarbon polymers as potential replacements for Nafion membranes, e.g. sulfonated polysulfone (SPSf) [5], sulfonated poly(aryl ether sulfone) (SPES) [6], sulfonated polyphosphazene (SPOP) [7], poly(benzimidazole) (PBI) [8], sulfonated polyimide (SPI) [9–12], and sulfonated poly(ether ether ketone) (SPEEK) [13-15]. Achieving high proton conductivity by increasing the degree of sulfonation usually results in a high degree of water induced swelling. Swelling tends to degrade the membrane's mechanical properties while increasing its permeability. Crosslinking is an efficient and simple approach to reducing both water uptake and methanol diffusion that also enhances the membrane's mechanical properties and dimensional stability. Numerous researchers have reported that while ionic and covalent cross-linked PEMs [10,13–21] show improved chemical and mechanical stabilities, their proton conductivity is reduced. Consequently, developing more efficient membranes with improved proton conductivities and reduced methanol crossover without adversely affecting their mechanical and chemical stabilities remains an important challenge. Proton transport in polymer membranes is a result of both vehicular diffusion and the Grotthuss shuttling mechanism [22]. When the temperature is above the boiling point of water, the loss of vehicular diffusion due to membrane dehydrated, results in significantly decreased proton conductivity. A strategy to develop proton conductive membranes for use in low humidity conditions has employed basic N-heterocycles (imidazole, pyrazole and triazole) [23-25], allowing Grotthuss proton conduction (i.e. non-vehicular mechanism), in which protons move from site to site without the assistance of the vehicular diffusion mechanism [26]. The nitrogen atoms in the heterocycles may act as donors and acceptors in proton transfer reactions [26], however, there is also an intermolecular proton transfer mechanism controlled by hydrogen bond breaking and formation.

Recently, the development of click chemistry [27] employing the highly efficient copper(I)-catalyzed Huisgen 1,3-dipolar cycloaddition [28,29] between azides and terminal alkynes has found popular appeal in the design of a variety of molecular architectures. The superior region-selectivity chemical pathway has the advantages of a short reaction time, a wide range of functionalities, a high yield, and tolerance toward humidity and oxygen [29]. The method has been used to synthesize a wide variety of linear, branched and cross-linked polymers [30–32].

Here we have focused on developing new materials that are capable of conducting protons under anhydrous conditions by the Grotthuss mechanism of proton transfer. Polymer membranes based on sulfonated polytriazole (SPTA) with different degrees of sulfonation with both acidic (sulfonic acid groups) and basic (triazole groups) in the polymer backbone were synthesized. The acid-base interactions between the basic N-heterocycles (triazole groups) and the sulfonic acid groups are able to form physical cross-linking sites in the SPTA electrolyte membranes. The SPTA membranes are expected to exhibit high conductivities in low humidity's, have adequate mechanical properties, and low methanol crossover.

2. Experimental section

2.1. Materials

Ethanol (≥99.5%, Sigma–Aldrich), N,N-Dimethylformamide (DMF) (99.8%, TEDIA), benzene (99.8%, Sigma–Aldrich), HCl (37%, Sigma–Aldrich), sodium hydroxide (≥97.0%, Sigma–Aldrich), potassium hydroxide (≥97.0%, Sigma–Aldrich), tetrabutylammonium bromide (99%, Sigma–Aldrich), sodium azide (≥99.0%, Sigma–Aldrich), anhydrous magnesium sulfate (99%, Sigma–Aldrich), copper(I) iodide (≥97%, Riedel-de Haën), 4,4′-Diazido-2,2′-stilbenedisulfonic acid, disodium salt hydrate (DADSDB) (97.0%, Sigma–Aldrich), potassium 2,5-dihydroxybenzenesulfonate (~75%, Sigma–Aldrich), bisphenol A (97%, Sigma–Aldrich), 1,2,3-1H-Triazole (97%, ACROS) and benzenesulfonic acid (90%, ACROS) were purchased and used as received. p-Xylylene dichloride (≥98.0%, Sigma–Aldrich) was recrystallized in methanol before used. Propargyl bromide (80 wt.% solution in toluene, Fluka) was distilled before used.

2.2. Preparation of monomers

2.2.1. 4,4′-(propane-2,2-diyl)bis((prop-2-ynyloxy)benzene) (PBPB) [33]

Bisphenol A (11.4 g, 50 mmol), sodium hydroxide (6 g, 150 mmol), deionized water, and tetrabutylammonium bromide (1.6 g, 5 mmol) were placed in a three-necked round bottom flask equipped with a magnetic stirrer, a reflux condenser, and a nitrogen gas inlet tube, after which the regents were heated to 80 °C. Propargyl bromide (14.87 g, 125 mmol) was added dropwise over 3 h and then the mixture was maintained at 80 °C for 10 h. The reaction product was washed several times with deionized water to remove tetrabutylammonium bromide and the salt formed in the reaction. The product was obtained through crystallization with ethyl alcohol.

Yield: 89%; mp = 78 °C; ^{1}H NMR ($CDCl_3$): δ = 1.68 (e), 2.53 (a), 4.68 (b), 6.89 (c), 7.17 (d) ppm (Figure S1); ^{13}C NMR ($CDCl_3$): δ = 31.54 (9), 42.26 (8), 55.99 (3), 75.68 (1), 79.25 (2), 114.47 (5), 128.20 (6), 144.37 (7), 155.61 (4) ppm (Figure S2).

2.2.2. 1,4-Bis(azidomethyl)benzene (BAB) [33]

p-Xylylene dichloride (8.8 g, 50 mmol), sodium azide (9.75 g, 150 mmol), DMF (100 mL), and benzene (100 mL) were added into a three-necked round bottom flask equipped with a magnetic stirrer and a reflux condenser. The reaction mixture was slowly heated to 80 °C and then maintained at that temperature for 12 h and then poured into a beaker containing deionized water (200 mL). The organic layer was separated following which the aqueous layer was extracted three times with benzene. The organic phases were combined and dried overnight ($MgSO_4$). Evaporation of the benzene yielded a light-yellow solid.

Yield: 83%; mp = 27–29 °C; ^{1}H NMR ($CDCl_3$): δ = 4.32 (b), 7.35 (a) ppm (Figure S3); ^{13}C NMR ($CDCl_3$): δ = 54.59 (1), 128.98 (3), 135.97 (2) ppm (Figure S4).

2.2.3. *Potassium 2,5-bis(prop-2-ynyloxy)benzenesulfonate (PBPBS)* [34]

Potassium 2,5-dihydroxybenzenesulfonate (5.00 g, 21.9 mmol), potassium carbonate (12.1 g, 87.5 mmol), and DMF (150 mL) were added into a three-necked round bottom flask with a magnetic stirrer, a reflux condenser and a nitrogen gas inlet tube. Propargyl bromide (10.4 g, 87.6 mmol) was then added dropwise into the flask at 80 °C for 3 h with stirring, after which the mixture was maintained at the same temperature for 2 d. Thereafter, the reaction mixture was washed several times with toluene to remove impurities. Recrystallization from a co-solvent of ethyl alcohol and deionized water yielded the yellow crystalline product.

Yield: 86%; ^{1}H NMR (DMSO-d_6): $\delta = 3.51$ (a), 4.74 (b), 6.96 (d), 7.04 (e), 7.35 (c) ppm (Figure S5); ^{13}C NMR (DMSO-d_6): $\delta = 55.98$ (10), 57.24 (3), 78.25 (1, 12), 79.5 (2,11), 115.65 (8), 116.59 (6), 116.77 (5), 137.86 (7), 148.5 (9), 151.02 (4) ppm (Figure S6).

2.3. *Synthesis of sulfonated polytriazole (SPTA)*

The SPTA was synthesized according to Scheme 1 through the click reaction with monomers and CuI (5 mol%) in DMF (15 wt.%) at 70 °C under a nitrogen atmosphere for 24 h. SPTA 1, SPTA 2 and SPTA 3 were synthesized with different monomers of PBPB, DADSDB, BAB and PBPBS in the molar ratios of 10:8:2:0, 10:10:0:0 and 8:10:0:2, respectively. After reaction, the copper salts were filtered and the SPTA powders were obtained by precipitation in methanol and purified in a Soxhlet extractor with methanol overnight and then dried at 60 °C in vacuo for at least 24 h. The structures and compositions of the SPTAs were determined by ^{1}H NMR as shown in Figures S7–S9 representing SPTA 1, SPTA 2 and SPTA 3, respectively. The degree of sulfonation and the calculated IEC_{th} values were quantitatively analyzed by using the integrated areas of the characteristic peaks in ^{1}H NMR (except for SPTA 3 whose characteristic peaks were overlapping). As shown in Figure S7 and S8, the sulfonation degree and the calculated IEC_{th} values of SPTA 1 and SPTA 2 were calculated by the integral areas ratio of peak "g, h" to peak "j, k" and peak "g, h" to peak "c, d", respectively.

2.4. *Film casting and membrane acidification*

The SPTA membranes were prepared through solution-casting and evaporation. SPTA powders were dissolved in DMF at room temperature as a 10 wt.% solution and cast onto a glass plate prior to heating at 60 °C for 48 h. Each membrane was soaked in methanol at room temperature to remove any residual solvent, and then peeled from the glass plate during immersion in deionized water. The SPTA membranes were obtained in acidic form by immersing them in aqueous HCl (1 M) for 24 h and then washing with deionized water until the pH was in the range 6–7.

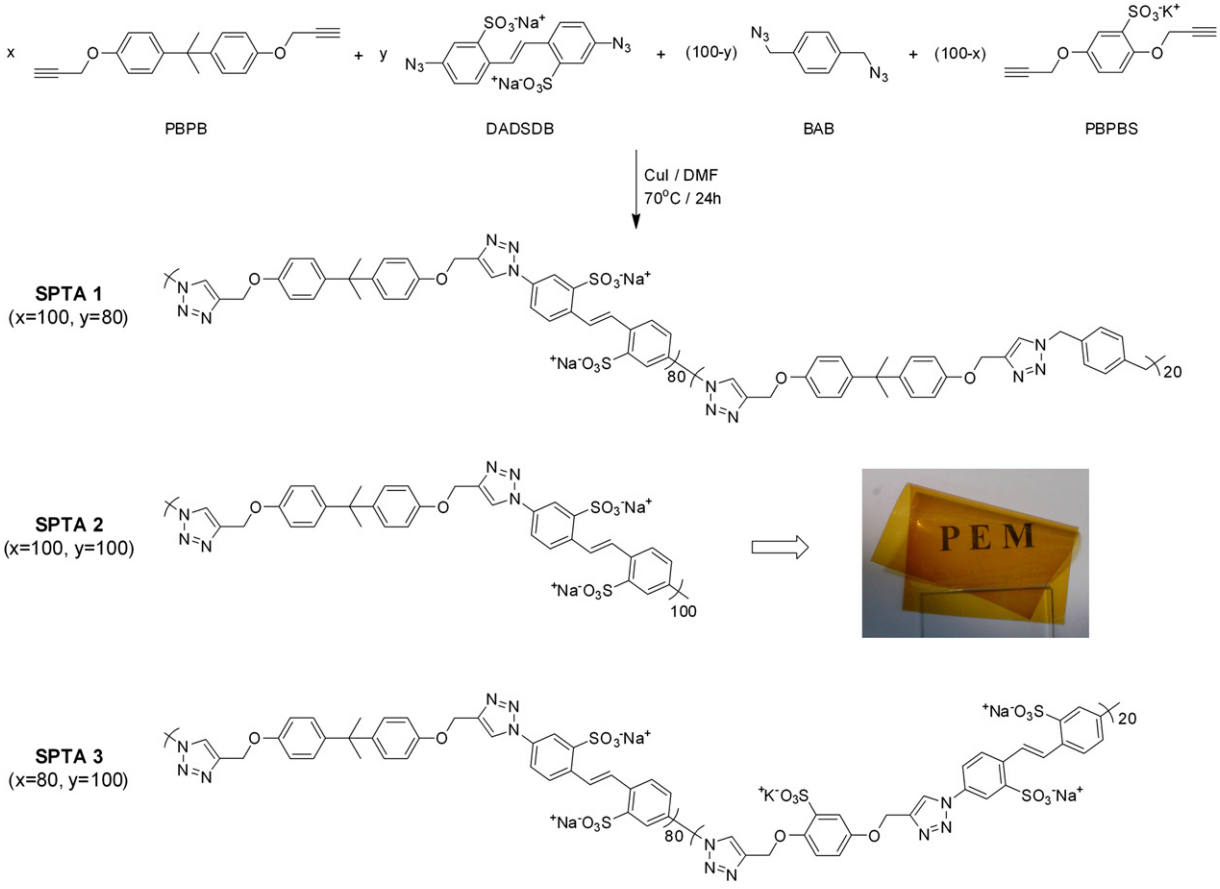

Scheme 1 – Synthesis routes of sulfonated polytriazole (SPTA) with different molar ratio monomers using the click reaction.

2.5. Immersion and freeze-drying process

Freeze-drying was used to study the morphology of the SPTA membranes after immersion in deionized water. Firstly, the membranes were immersed in deionized water for 1 day and then immediately frozen by immersing for 10 min in liquid nitrogen at −195 °C. Finally, the icy layer that covered the polymer surface was progressively removed by sublimation at low temperature (−170 °C), for 1 h; during which time the pressure and the temperature were increased to 1.0×10^{-4} Torr and to −30 °C, respectively, to remove the residual water content.

2.6. Membrane characterizations

NMR spectra were recorded at 25 °C on an INOVA 500 MHz NMR spectrometer. FT-IR spectra were recorded on a Nicolet Avatar 320 FT-IR spectrophotometer from 4000 to 400 cm^{-1} at a resolution of 1.0 cm^{-1} under a continuous nitrogen flow. The thermal degradation behavior of the membranes was measured using a Q50 thermogravimetric analyzer (TGA) operated from room temperature to 850 °C at a heating rate of 20 °C min^{-1} under a nitrogen atmosphere. The glass transition temperature (T_g) was measured using differential scanning calorimetry (DSC) with a DuPont TA Instrument Q20 controller. Dynamic mechanical thermal analysis (DMTA) was performed using a DMA/SDTA861^e dynamic mechanical analyzer (DMA). The tensile properties were measured according to ASTM 638 on a Shimadzu AG-50kNE universal tester at a crosshead speed of 1 mm/min. The membrane morphologies were characterized using a JEOL TEM-1200EX-II instrument operated at 120 kV. To stain the hydrophilic domains, the membranes were converted into their Pb^{2+} forms by immersing in $Pb(AC)_2$ (Lead acetate, 1 N) solution overnight and then rinsing with water. Membranes were dried under vacuum at 80 °C for 12 h and then sectioned into 50 nm slices using an ultramicrotome. The slices were picked up with 200 mesh copper grids for TEM observation. Wide-angle X-ray diffraction (WAXD) spectra were recorded on powdered samples using a Rigaku D/max-2500 type X-ray diffraction instrument.

The water uptake (WU; %) was calculated using Eq. (1) [14]:

$$WU(\%) = \frac{W_{wet} - W_{dry}}{W_{dry}} \times 100\% \quad (1)$$

The dried SPTA membranes were immersed in deionized water at room temperature for 24 h, then removed quickly and blotted with filter paper to remove any excess surface water, and immediately weighed to obtain their wet masses (W_s). The membranes were then dried at 120 °C for 24 h to determine their dry weights (W_d).

The ion exchange capacities (IECs) were determined by titrating (with aqueous NaOH) the protonic form of the membrane generated after ion-exchange treatment with 1 M NaCl. The ionic concentration was calculated using Eq. (2) [14]:

$$[H^+] = \frac{IEC \times W_d/V_W}{1000} \quad (2)$$

where IEC refers to the titrated IEC, W_d is the weight of the dry membrane, and V_w is the volume of the wet membrane.

The number of water molecules per ionic group, λ, was determined using Eq. (3) [14]:

$$\lambda = \frac{WU}{18 \times IEC} \quad (3)$$

The amount of free water in the fully hydrated membranes was determined using a DuPont TA2010 differential scanning calorimeter. The samples were first cooled from 25 to −60 °C and then heated to 50 °C at a rate of 5 °C min^{-1}. The mass of free water in the membranes was measured by integrating the area under the cooling curve and comparing it to the measured enthalpy of fusion for water (314 J/g).

The proton conductivity of the membrane was determined with an ac electrochemical impedance analyzer (PGSTAT 30), the ac frequency being scanned from 100 kHz to 10 Hz at a voltage amplitude of 10 mV. The membrane (1 cm in diameter) was sandwiched between two smooth stainless steel disk electrodes in a cylindrical PTFE holder. The proton conductivity was calculated according to Eq. (4) [14]:

$$\sigma = \frac{L}{RA} \quad (4)$$

Where: σ is the proton conductivity (in S cm^{-1}), L is the distance between the electrodes, A is the membrane section area (in cm^2), and R is the impedance of the membrane (in ohms).

Water desorption measurements were performed using a TGA Q50 to determine weight changes over time at 80 °C. The water diffusion coefficient was calculated according to Eq. (5) [14]:

$$\frac{M_t}{M_\infty} = 4\left(\frac{D_t}{\pi L^2}\right)^{1/2} \quad (5)$$

Where: D is the water diffusion coefficient, M_t/M_∞ represents the water desorption, and L is the membrane thickness.

The methanol diffusion coefficient of the membrane was measured using a two-chamber liquid permeability cell. The description of this cell has been described in detail previously [35]. The methanol concentrations in the water cell were determined periodically using a GC-8A gas chromatograph (SHTMADU, Tokyo, Japan). The methanol permeability was calculated using Eq. (6) [14]:

$$C_B(t) = \frac{A}{V_B}\frac{P}{L}C_A(t - t_0) \quad (6)$$

Where: L is the membrane thickness, A is the membrane area, C_A and C_B are the methanol concentrations in the methanol and water chambers, respectively, and P is the methanol diffusion coefficient.

3. Results and discussion

3.1. Interactions of 1,2,3-1H-triazole and benzenesulfonic acid

As mentioned in the introduction, the presence of acid-base interactions can reduce the degree of water uptake, methanol diffusion and enhance the mechanical properties of PEMs. However, acid-base interactions in the polymer matrix

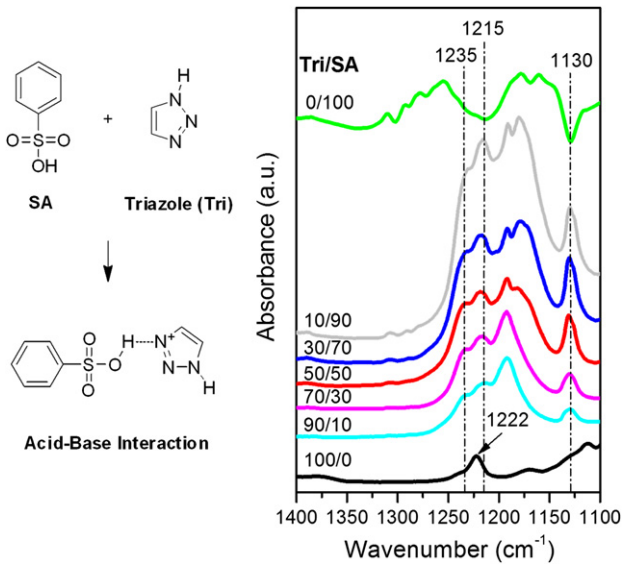

Fig. 1 – FT-IR spectra for blending of sufonic acid (SA) and triazole (Tri).

are difficult to observe due to the overlap of the absorption peaks. In order to investigate the interactions we designed a model system. 1,2,3-1H-triazole has significant structural homology with the triazole derivative in the SPTA polymers; thus, we blended 1,2,3-1H-triazole and benzenesulfonic acid monomers to observe the acid-base interactions. Although the structure of the 1,2,3-1H-triazole monomer contains both a tertiary amine and a secondary amine (N–H) and is different from the triazole derivative in the SPTA polymer, which contains only a tertiary amine, this difference should not interfere with the observation of the acid-base interactions between the sulfonic acid ($-SO_3^-$ group) and the triazole (tertiary amine group). FT-IR spectra were taken to confirm the acid-base interactions between the sulfonic acid and triazole as shown in Fig. 1. The broad absorption band near 1200 cm^{-1} is attributed to an asymmetric O=S=O stretching vibration of the $-SO_3^-$ groups [36]. Fig. 1 shows the spectral changes that are due to the presence of the benzenesulfonic acid monomer, they can be described as follows: (i) the intensity increase of the peak at 1130 cm^{-1} is attributed to the deprotonation of the sulfonic acid group ($-SO_3^-$) [36], (ii) the absorption band at 1222 cm^{-1} representing self-association of N–H…N i.e. inter-molecular hydrogen bonding (dimers) is split into two bands at 1215 cm^{-1} and 1235 cm^{-1}, due to the interaction between sulfonic acid ($-SO_3H$) and triazole (N–H), and free N–H absorption. Based on FT-IR results from the model mixture, similar acid-base interactions in the polymer matrix can be expected and thus regarded as being a physical crosslinking site. The presence of these interactions results in the formation of well-dispersed ionic clusters and the random distribution of ion channels with good connectivity.

3.2. *Morphologies of SPTA membranes*

The sulfonated membrane with uniform ionic clusters displays improved proton conductivity and methanol permeability due to the smaller dimensions and the connectedness of the transport channels [37]. Fig. 2 shows TEM micrographs of SPTA membranes where the darker regions represent localized hydrophilic ionic clusters and the lighter parts represent hydrophobic moieties. The SPTA 1 membrane possesses uniform ionic clusters from a few nm to 50 nm due to better hydrophilic/hydrophobic distribution within the SPTA 1 membrane. The existence of acid-base interactions between sulfonic acid and triazole enhances the random distribution, and hence connectivity, of ion channels, while preventing the aggregation of hydrophilic sulfonic acid groups into larger ionic clusters. Nevertheless, the increased degree of sulfonation causes a slight aggregation of the hydrophilic phase resulting in some large ionic clusters but overall the phase remains well-dispersed.

It is well known that the size distribution of the ionic channels directly affects the methanol permeability of the membrane. Although XRD has been widely used to estimate the size of the ionic channels in sulfonated polymers, it may not give an accurate representation of the membranes when in use because the membranes investigated by XRD were in a non-hydrated state. In the present study, freeze-drying (in

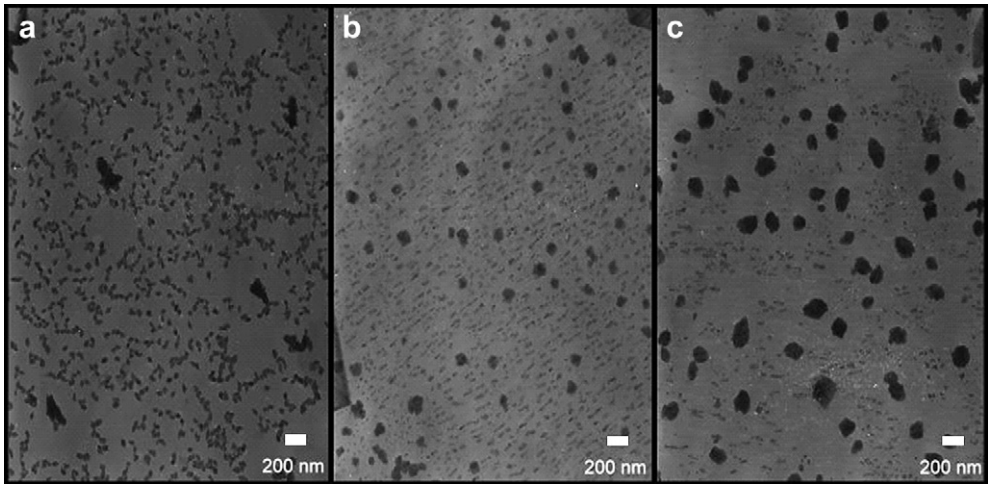

Fig. 2 – TEM micrographs of (a) SPTA 1 (b) SPTA 2 and (c) SPTA 3 membranes.

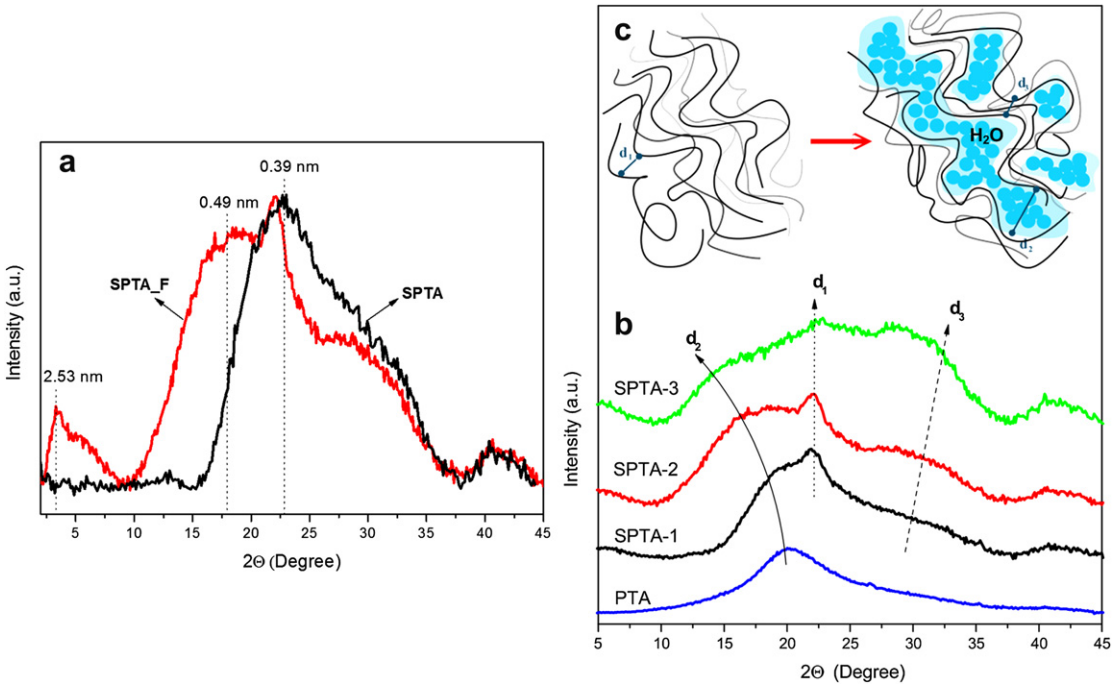

Fig. 3 – Wide-angle X-ray diffraction patterns of (a) the hydrated state SPTA 2 membrane after freeze-drying (red) compared with dry state (black) and (b) the hydrated state of the SPTA membranes after freeze-drying process. (c) Illustration of the distance between the polymer chain at dry state (left) and hydrated state (right). (For interpretation of the references to colour in this figure legend, the reader is referred to the web version of this article.)

liquid nitrogen) was used to preserve the morphology of the hydrated sulfonated polymer membranes.

Fig. 3(a) shows XRD patterns of SPTA 2 after freeze-drying and in the dry state. The amorphous peak of the SPTA 2 membrane ($2\theta = 22.8^\circ$) was shifted to a slightly lower value and a new broad amorphous peak at $2\theta = 3.4^\circ$ appeared after freeze-drying, an indication of larger ionic channel sizes in water swollen membranes. The change in the ionic channel size of the SPTA membranes induced by freeze-drying can be obtained from the XRD patterns. As shown in Fig. 3(b), a comparison of the XRD patterns of the non-sulfonated polymer (PTA) [33] with the sulfonated polymer (SPTA) reveals that the amorphous peak near $2\theta = 20.0^\circ$ (i.e. the inter-molecular main chain spacing distance [38,39]) shifts lower and a new amorphous peak at $2\theta = 29.8^\circ$ (i.e. the intra-molecular main chain spacing distance [38,39]) appears with an increasing degree of sulfonation. The larger sizes of ionic clusters in the membranes are more favorable for water swelling, therefore, we presume that they tend to expand the inter-molecular main chain spacing (d_2) and reduce the intra-molecular distance (d_3) between the rigid polymer backbones as shown in the illustration in Fig. 3(c) [33,40,41]. The change in size of the ionic channel in the membranes is an important factor affecting the methanol crossover through the electrolyte membrane that will be discussed later.

Table 1 – IEC, WU and λ values of SPTA membranes.

Code	Ion exchange capacity (meq/g)			Water uptake (wt.%)[d]	λ (H_2O/SO_3H)
	Calculated IEC_{th}[a]	Calculated IEC_{th}[b]	Titration IEC_{tit}[c]		
SPTA 1	2.35	2.28	2.21	26.1	6.6
SPTA 2	2.59	2.55	2.43	35.7	8.2
SPTA 3	2.86	–	2.73	51.5	10.5
SPI	2.20	2.19	1.99	76.4	21.3
SPEEK	–	2.06	1.99	53.2	14.9
Nafion 117	0.92	–	0.78	35.6	25.4

a IEC calculated from feed monomer ratio.
b IEC calculated from ^{1}H NMR.
c IEC measured with titration.
d Measured at 30 °C.

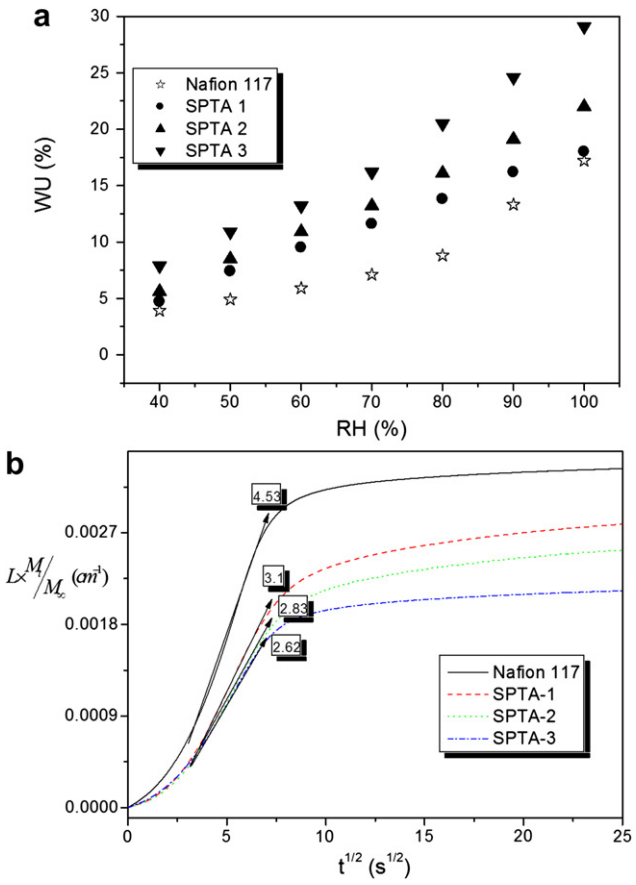

Fig. 4 – (a) The WU of Nafion 117 and SPTA membranes at 60 °C as a function of RH. (b) The water desorption of Nafion 117 and SPTA membranes. The numbers in the boxes correspond to the water diffusion coefficients ($\times 10^{-5}$ cm^{-2} s^{-1}).

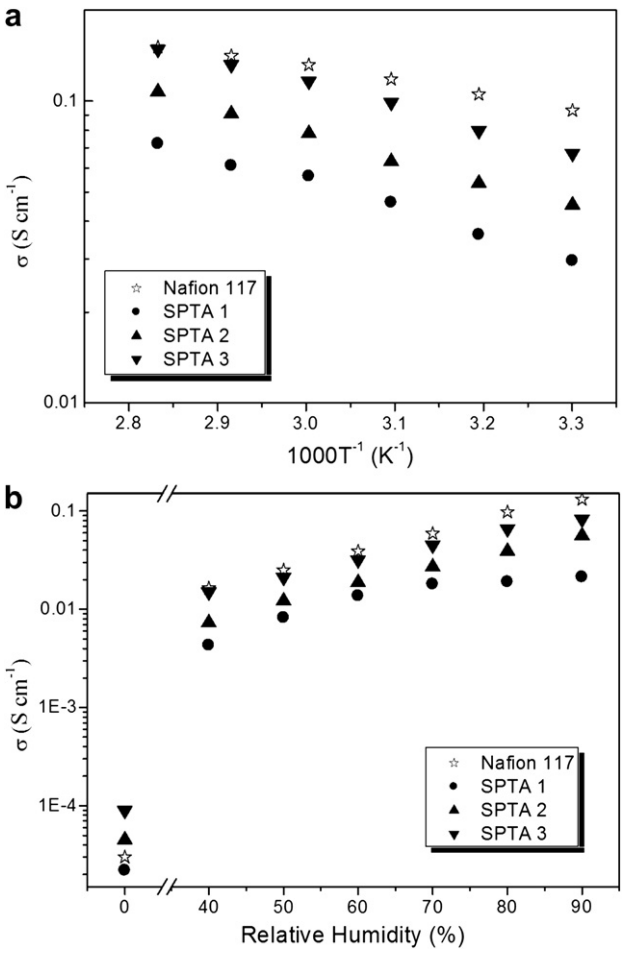

Fig. 5 – (a) Proton conductivities of Nafion 117 and SPTA membranes as function of the temperature at 90 RH. (b) Proton conductivities of Nafion 117 and SPTA membranes as function of the RH at 60 °C.

3.3. *Ionic exchange capacity (IEC) and water behaviors*

Previous studies have indicated that the formation of the acid-base complexes within PEMs give rise to perturbations when measuring the IEC. This results from the exchange of the acid protons in the PEMs being comparatively more difficult than with other sulfonated polymers [19]. To eliminate this effect, the membrane was kept in the titration solution until the measurement was completed. Table 1 lists the water uptake (WU), ionic exchange capacity (IEC) and corresponding lambda values (λ) of Nafion 117 and SPTA membranes. The IEC values of the SPTA membranes ranged from 2.21 to 2.73 mequiv g^{-1}. The increase in IEC value with the increase in sulfonic acid content is due to the increase in the overall sulfonic acid content. The high IEC implies the presence of sufficient "free" sulfonic groups for proton transport.

The WU of sulfonated polymers is known to have a profound effect on membrane conductivity and mechanical properties [2]. Excessive WU will induce undesired side effects such as membrane swelling, mechanical frailty, low dimensional stability and high methanol permeability and lead to poor performance in DMFC applications. Higher IEC values are generally accompanied by higher WU. As expected, the WU of the SPTA membrane increases with increasing IEC values. Lower λ values for SPTA 1 ($\lambda = 6.6$) were noted in comparison to other sulfonated derivatives of aromatic polymer membranes ($\lambda = 21.3$) [10,14] with similar IEC values (Table 1). As described above (Section 1), the acid-base interactions in the SPTA matrix effectively act as a physical crosslinking mechanism that reduces membrane swelling and λ values. The results demonstrated that the combination of acid and base groups in the polymer backbone is an effective approach for controlling WU and depressing membrane swelling in water. The relationship between the WU and RH at 60 °C is shown in Fig. 4(a) where the increase of the WU is less dramatic with the increase of sulfonation degree in the SPTA membranes. A possible explanation is that the greater number of sulfonic acid groups increases the acid-base interactions in triazole-based polymer matrix.

Water retention and diffusion in PEMs has a significant effect on proton conductivity, especially at high temperatures and low RH. The water retention and diffusion of membranes provides indirect evidence for the variation in the WU with increases in temperature and a reduction in RH. The water desorption curves of the SPTA membranes are shown in

Table 2 – Methanol uptake, proton conductivity, methanol permeability, and selectivity of the Nafion 117 and SPTA membranes.

Code	Methanol uptake (wt.%)[a]	Proton conductivity σ (S cm^{-1})[b]		Methanol permeability P ($\times 10^{-6}$ cm^2 s^{-1})[a]	Selectivity $\Phi \times 10^5$ (S cm^{-3} s)
		σ_{30} at 30 °C	σ_{80} at 80 °C		Φ_{30} (σ_{30}/P)
SPTA 1	19.2	0.030	0.072	0.1	3.00
SPTA 2	25.0	0.045	0.107	0.45	1.00
SPTA 3	28.8	0.067	0.149	0.61	1.10
Nafion 117	62.1	0.093	0.151	1.31	0.71

a Measured at 30 °C.
b Measured at 90 RH.

Fig. 4(b): they show that the velocity of water volatilization was slightly reduced with an increase in the degree of sulfonation. These findings are in good agreement with the relationship between the WU and the RH data mentioned above.

3.4. *Proton conductivity and methanol permeability*

Proton conductivities (σ) of SPTA membranes at different temperatures (30–80 °C) with 90% RH are shown in Fig. 5(a) with the extracted data being summarized in Table 2. The proton conductivities of all the membranes are higher than 0.01 S cm^{-1}, which is the lowest value required for practical application as PEMs in fuel cells. Two mechanisms may be involved in proton transportation, the Grotthuss mechanism [22] based mainly on 'hopping' and the vehicle mechanism based mainly on the diffusion of H_3O^+ ions - any increase in temperature will strongly enhance both mechanisms. For comparison, a previous report by Boaventura et al. for heterocycle-based proton exchange membranes doped with agents such as 1H-benzimidazole-2-sulfonic acid and phosphoric acid, showed the conductivity not to be significantly influenced by temperature [42]. Similar behavior was observed by Gomes et al. [43,44] and may be due to the high stiffness of the doped proton exchange membranes within the temperature range studied. In our work, conductivity was found to be significantly influenced by temperature. Fig. 5(a) shows that the proton conductivities of all the SPTA membranes increased with temperature and the IEC value. This result is in agreement with the general rule that the ionic conductivity of an ion-exchange membrane is strongly related to its temperature and water content.

More information related to the proton conductivity of the SPTA membranes can be gained by examining its relationship to RH. In our work, the proton conductivity was significantly influenced by RH. By examining proton conductivity as a function of RH at 60 °C (Fig. 5(b)), it is apparent that for all the SPTA membranes proton conductivity significantly as the RH decreases: this is a phenomenon that has been commonly

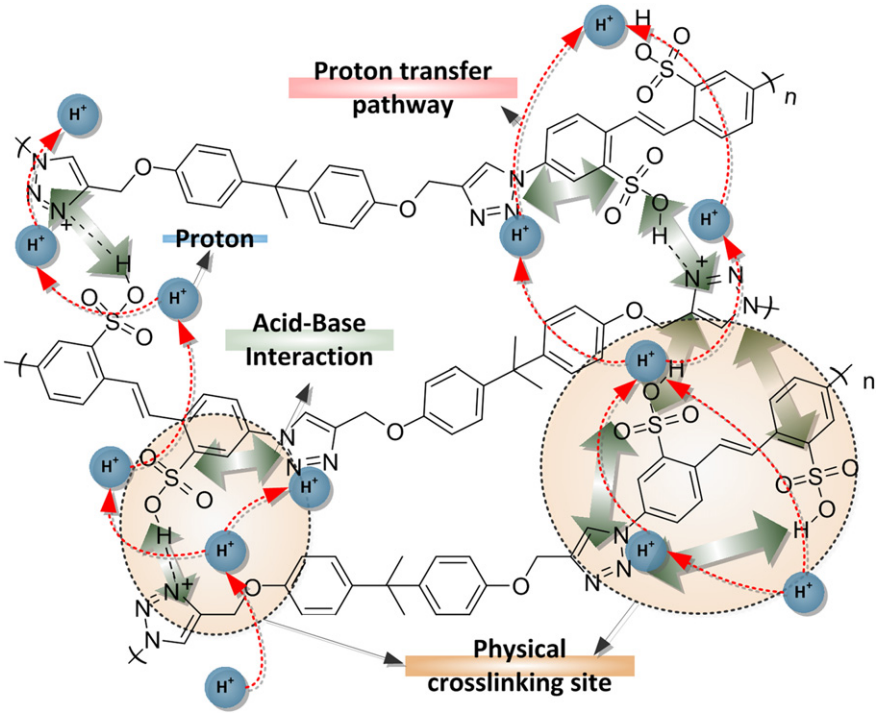

Fig. 6 – Proposed proton-conducting mechanism in SPTA membranes.

Table 3 – The thermal and mechanical properties of Nafion and SPTA membranes.

Code	T_{d5}	Tensile strength (MPa)[a]	Young's modulus (GPa)[a]	Elongation at break (%)[a]	Storage modulus (MPa)[a]
SPTA 1	254.1	28.2	4.57	8.23	2567
SPTA 2	247.2	24.7	4.38	7.05	2447
SPTA 3	245.6	21.3	4.08	5.94	1851
Nafion	–	28.4[b]	0.1[b]	329[b]	<1000[c]

a Measured in the hydrated state.
b According to ref. [46].
c According to ref. [47].

observed with many other sulfonated polymer membranes. It should be noted that the reduction of SPTA proton conductivity is less dramatic than that of Nafion 117, due to the fact that the SPTA membranes exhibit better water retention capability than Nafion 117. In addition, when the proton conductivity was measured at a low RH proton transport depended strongly on the distance between the hopping sites. The presence of the ionic interactions in the membrane (Section 3.1.) induces the formation of random proton conductive pathways to facilitate proton transfer [8,45], thereby enhancing proton conductivity at low RH. However, the physically cross-linked SPTA membranes have acidic and basic sites that are able to facilitate proton transfer, the site-to-site jumping distances are minimized and the transfer process is facilitated at low RH [24]. TEM micrographs of the SPTA membranes (Fig. 2) also indicate that introduction of the triazole groups in the membrane results in a better distribution of the ionic clusters. Fig. 6 shows a possible proton-conducting scheme in the SPTA membranes where proton hopping from sulfonic acid groups to 1,2,3-triazole groups occurs; a similar mechanism has been proposed by other workers [24].

Methanol permeability is an important consideration in DMFC applications, since the crossover of methanol from the anode to the cathode leads to a lower cell voltage and decreased fuel efficiency. Table 2 shows the methanol uptake and the methanol diffusion coefficients of the SPTA membranes and Nafion 117 at 30 °C. As mentioned above (Section 3.2), a high WU will induce high methanol uptake and high methanol permeability. Table 1 shows that the WU of SPTA membranes increases with increasing sulfonation, resulting in an increase in both methanol uptake and methanol permeability. Although both methanol uptake and permeability increase with WU it is important to note that the water uptakes of SPTA 2 and 3 are both higher than that of Nafion 117, while the methanol uptakes and permeabilities are both lower (Table 2). This is due to the presence of acid-base interactions in the SPTA matrix acting as physical crosslinking sites that suppress membrane swelling resulting in a reduction of WU.

In practical use PEMs in DMFCs, need to exhibit high proton conductivities and low methanol permeabilities. The ratio of the proton conductivity to the methanol permeability, Φ, is an effective parameter for evaluating the membrane's performance. Table 2 shows the selectivity of the SPTA membranes, defined as the ratio of proton conductivity at 30 °C to methanol permeability. All SPTA membranes exhibit better selectivity compared to Nafion 117, especially the SPTA 1 membrane that has a selectivity about three times higher than Nafion 117.

3.5. *Thermal and mechanical properties*

Table 3 summarizes the dynamic mechanical thermal analysis (DMTA) results, and the thermal and mechanical properties of SPTA membranes. The temperatures for thermal weight losses (T_{d5}) were in the range 245.6–254.1 °C, no glass transition temperature (T_g) was observed for any of the SPTA membranes in the temperature range 50–350 °C using DSC or DMA.

It is essential for PEMs to possess adequate mechanical integrity to withstand fabrication of the membrane electrode assembly. When subjected to hot pressing, the electrodes can potentially peel away from the MEA due to membrane deformation. The experimental results: i.e. Young's modulus, tensile strength, elongation properties and storage modulus of the SPTA membranes at room temperature are summarized in Table 3. The membranes showed superior mechanical properties, when compared to Nafion [46,47], with storage modulus values of 1851–2567 MPa, elongation at break values of 5.94–8.23% and Young's modulus values of 4.08–4.57 GPa. The tensile strength values were in the range of 21.3–28.2 MPa.

4. Conclusions

In conclusion, we have successfully synthesized a new proton exchange membrane by employing the click reaction with sulfonated polytriazole (SPTA), in which noncovalent interactions mediate physical crosslinking between the acidic (sulfonic acid) and basic (triazole) groups in the polymer's backbone. Acid-base interactions are responsible for the well-dispersed nature of the ionic clusters that lead to the random distribution of well-connected ion channels. The SPTA membranes possess uniformly distributed conductive sites resulting in better proton conduction. This is facilitated by the N-heterocycles being dispersed throughout the polymer that facilitate high proton conductivity at elevated temperatures or at low relative humidities. The acid-base interactions lead to the suppression of membrane swelling and the reduction of WU leading to lower methanol permeability. The selectivity of the SPTA membranes ranges between one and four times that of Nafion 117, thus implying their potential for practical applications in DMFCs.

Acknowledgments

This study was support financially by the National Science Council, Taiwan (contract no. NSC-98-2218-E-009-001).

Appendix. Supplementary data

Supplementary data related to this article can be found online at doi:10.1016/j.ijhydene.2011.08.093.

REFERENCES

[1] Steele B-C-H, Heinzel A. Materials for fuel-cell technologies. Nature 2001;414:345–52.
[2] Hickner M-A, Ghassemi H, Kim Y-S, Einsla B-R, McGrath J- E. Alternative polymer systems for proton exchange membranes (PEMs). Chemical Reviews 2004;104:4587–612.
[3] Mauritz K-A, Moore R- B. State of understanding of nafion. Chemical Reviews 2004;104:4535–86.
[4] Wang C-Y. Fundamental models for fuel cell engineering. Chemical Reviews 2004;104:4727–66.
[5] Fu Y-Z, Manthiram A. Synthesis and characterization of sulfonated polysulfone membranes for direct methanol fuel cells. Journal of Power Sources 2006;157:222–5.
[6] Miyatake K, Chikashige Y, Higuchi E, Watanabe M. Tuned polymer electrolyte membranes based on aromatic polyethers for fuel cell applications. Journal of the American Chemical Society 2007;129:3879–87.
[7] Peighambardoust S-J, Rowshanzamir S, Amjadi M. Review of the proton exchange membranes for fuel cell applications. International Journal of Hydrogen Energy 2010;35:9349–84.
[8] Jouanneau J, Mercier R, Gonon L, Gebel G. Synthesis of sulfonated polybenzimidazoles from functionalized monomers: preparation of ionic conducting membranes. Macromolecules 2007;40:983–90.
[9] Asano N, Aoki M, Suzuki S, Miyatake K, Uchida H, Watanabe M. Aliphatic/aromatic polyimide ionomers as a proton conductive membrane for fuel cell applications. Journal of the American Chemical Society 2006;128:1762–9.
[10] Ye Y-S, Huang Y-J, Cheng C-C, Chang F-C. A new supramolecular sulfonated polyimide for use in proton exchange membranes for fuel cells. Chemical Communications 2010;46:7554–6.
[11] Tseng C-Y, Ye Y-S, Joseph J, Kao K-Y, Rick J, Huang S-L, et al. Tuning transport properties by manipulating the phase segregation of tetramethyldisiloxane segments in modified polyimide electrolytes. Journal of Power Sources 2011;196: 3470–8.
[12] Leila A-F, Shahram M-A, Hamid Y. Survey of sulfonated polyimide membrane as a good candidate for nafion substitution in fuel cell. International Journal of Hydrogen Energy 2010;35:9385–97.
[13] Zhong S, Cui X, Cai H, Fu T, Zhao C, Na H. Crosslinked sulfonated poly(ether ether ketone) proton exchange membranes for direct methanol fuel cell applications. Journal of Power Sources 2007;164:65–72.
[14] Ye Y-S, Yen Y-C, Cheng C-C, Chen W-Y, Tsai L-T, Chang F-C. Sulfonated poly(ether ether ketone) membranes crosslinked with sulfonic acid containing benzoxazine monomer as proton exchange membranes. Polymer 2009;50:3196–203.
[15] Han M, Zhang G, Li M, Wang S, Zhang Y, Li H, et al. Considerations of the morphology in the design of proton exchange membranes: cross-linked sulfonated poly(ether ether ketone)s using a new carboxyl-terminated benzimidazole as the cross-linker for PEMFCs. International Journal of Hydrogen Energy 2011;36:2197–206.
[16] Thomas O-D, Peckham T-J, Thanganathan U, Yang Y, Holdcroft S. Sulfonated polybenzimidazoles: proton conduction and acid–base crosslinking. Journal of Polymer Science Part A: Polymer Chemistry 2010;48:3640–50.
[17] Lee K-S, Jeong M-H, Lee J-P, Lee J-S. End-group cross-linked poly(arylene ether) for proton exchange membranes. Macromolecules 2009;42:584–90.
[18] Wu D, Xu T, Wu L, Wu Y. Hybrid acid-base polymer membranes prepared for application in fuel cells. Journal of Power Sources 2009;186:286–92.
[19] Ye Y-S, Chen W-Y, Huang Y-J, Cheng M-Y, Yen Y-C, Cheng C-C, et al. Preparation and characterization of high-durability zwitterionic crosslinked proton exchange membranes. Journal of Membrane Science 2010;362:29–37.
[20] Zhao C, Lin H, Na H. Novel cross-linked sulfonated poly (arylene ether ketone) membranes for direct methanol fuel cell. International Journal of Hydrogen Energy 2010;35: 2176–82.
[21] Zhang Y, Fei X, Zhang G, Li H, Shao K, Zhu J, et al. Preparation and properties of epoxy-based cross-linked sulfonated poly(arylene ether ketone) proton exchange membrane for direct methanol fuel cell applications. International Journal of Hydrogen Energy 2010;35:6409–17.
[22] Kreuer K-D, Paddison S-J, Spohr E, Schuster M. Transport in proton conductors for fuel-cell applications: simulations, elementary reactions, and phenomenology. Chemical Reviews 2004;104:4637–78.
[23] Zhou Z, Li S, Zhang Y, Liu M, Li W. Promotion of proton conduction in polymer electrolyte membranes by 1H-1,2,3-triazole. Journal of the American Chemical Society 2005;127: 10824–5.
[24] Ponce M-L, Boaventura M, Gomes D, Mendes A, Madeira L-M, Nunes S-P. Proton conducting membranes based on benzimidazole sulfonic acid doped sulfonated poly(oxadiazole–triazole) copolymer for low humidity operation. Fuel Cells 2008;8:209–16.
[25] Jithunsa M, Tashiro K, Nunes S-P, Chirachanchai S. Poly(acrylic acid-co-4-vinylimidazole)/sulfonated poly(ether ether ketone) blend membranes: a role of polymer chain with proton acceptor and donor for enhancing proton transfer in anhydrous system. International Journal of Hydrogen Energy 2011;36:10384–91.
[26] Kreuer K-D. Proton conductivity: materials and applications. Chemistry of Materials 1996;8:610–41.
[27] Kolb H-C, Finn M-G, Sharpless K-B. Click chemistry: diverse chemical function from a few good reactions. Angewandte Chemie International Edition 2001;40:2004–21.
[28] Huisgen R. Cycloadditions — definition, classification, and characterization. Angewandte Chemie International Edition in English 1968;7:321–8.
[29] Rostovtsev V-V, Green L-G, Fokin V-V, Sharpless K-B. A stepwise huisgen cycloaddition process: copper(I)-catalyzed regioselective "ligation" of azides and terminal alkynes. Angewandte Chemie International Edition 2002;41:2596–9.
[30] Wu P, Feldman A-K, Nugent A-K, Hawker C-J, Scheel A, Voit B, et al. Efficiency and fidelity in a click-chemistry route to triazole dendrimers by the copper(I)-catalyzed ligation of azides and alkynes. Angewandte Chemie International Edition 2004;43:3928–32.
[31] Scheel A-J, Komber H, Voit B-I. Novel hyperbranched poly([1,2,3]-triazole)s derived from AB2 monomers by a 1,3-dipolar cycloaddition. Macromolecular Rapid Communications 2004;25:1175–80.
[32] Agut W, Taton D, Lecommandoux S. A versatile synthetic approach to polypeptide based rod–coil block copolymers by click chemistry. Macromolecules 2007;40:5653–61.

[33] Ye Y-S, Yen Y-C, Cheng C-C, Syu Y-J, Huang Y-J, Chang F-C. Polytriazole/clay nanocomposites synthesized using in situ polymerization and click chemistry. Polymer 2010;51:430–6.
[34] Ye Y-S, Cheng M-Y, Tseng J-Y, Liang G-W, Rick J, Huang Y-J, et al. New proton conducting membranes with high retention of protic ionic liquids. Journal of Materials Chemistry 2011;21:2723–32.
[35] Lin C-W, Huang Y-F, Kannan A-M. Semi-interpenetrating network based on cross-linked poly(vinyl alcohol) and poly(styrene sulfonic acid-co-maleic anhydride) as proton exchange fuel cell membranes. Journal of Power Sources 2007;164:449–56.
[36] Bozkurt A. Anhydrous proton conductive polystyrene sulfonic acid membranes. Turkish Journal of Chemistry 2005; 29:117–23.
[37] Li X, Zhang G, Xu D, Zhao C, Na H. Morphology study of sulfonated poly(ether ether ketone ketone)s (SPEEKK) membranes: the relationship between morphology and transport properties of SPEEKK membranes. Journal of Power Sources 2007;165:701–7.
[38] Wu J, Haddad T-S, Kim G-M, Mather P-T. Rheological behavior of entangled polystyrene–polyhedral oligosilsesquioxane (POSS) copolymers. Macromolecules 2007;40:544–54.
[39] Cheng C-C, Huang C-F, Yen Y-C, Chang F-C. A "plug and play" polymer through biocomplementary hydrogen bonding. Journal of Polymer Science Part A: Polymer Chemistry 2008;46:6416–24.
[40] Norimitsu T-Y-I, Mikiji M, Nobuyoshi Y, Eiko M, Yasushi K. Photoreactive and inactive crystals of 1-alkylthymine derivatives. Bulletin of the Chemical Society of Japan 1999;72: 851–8.
[41] Ye Y-S, Yen Y-C, Chen W-Y, Cheng C-C, Chang F-C. A simple approach toward low-dielectric polyimide nanocomposites: blending the polyimide precursor with a fluorinated polyhedral oligomeric silsesquioxane. Journal of Polymer Science Part A: Polymer Chemistry 2008;46:6296–304.
[42] Boaventura M, Ponce M-L, Brandão L, Mendes A, Nunes S-P. Proton conductive membranes based on doped sulfonated polytriazole. International Journal of Hydrogen Energy 2010; 35:12054–64.
[43] Gomes D, Roeder J, Ponce M-L, Nunes S-P. Characterization of partially sulfonated polyoxadiazoles and oxadiazole-triazole copolymers. Journal of Membrane Science 2007;295:121–9.
[44] Gomes D, Roeder J, Ponce M-L, Nunes S-P. Single-step synthesis of sulfonated polyoxadiazoles and their use as proton conducting membranes. Journal of Power Sources 2008;175:49–59.
[45] Zhang F, Li N, Cui Z, Zhang S, Li S. Novel acid-base polyimides synthesized from binaphthalene dianhydrie and triphenylamine-containing diamine as proton exchange membranes. Journal of Membrane Science 2008;314:24–32.
[46] Liu B, Robertson G-P, Kim D-S, Guiver M-D, Hu W, Jiang Z. Aromatic poly(ether ketone)s with pendant sulfonic acid phenyl groups prepared by a mild sulfonation method for proton exchange membranes†. Macromolecules 2007;40: 1934–44.
[47] Kundu S, Simon L-C, Fowler M, Grot S. Mechanical properties of nafion(TM) electrolyte membranes under hydrated conditions. Polymer 2005;46:11707–15.